Astron. Astrophys. 250, L5–L8 (1991)

ASTRONOMY AND ASTROPHYSICS

Letter to the Editor

MG1131+0456: discovery of the optical Einstein ring with the NTT

F. Hammer[1], O. Le Fèvre[1,2], M.C. Angonin[1], G. Meylan[3], A. Smette[4], and J. Surdej[5,]**

[1] DAEC, Observatoire de Paris-Meudon, F-92195 Meudon Cedex, France
[2] Canada-France-Hawaii Telescope Corporation, P.O. Box 1597, Kamuela, HI 96743, USA
[3] Space Telescope Science Institute, 3700 San Martin Dr., Baltimore, MD 21218-301, USA
[4] European Southern Observatory, Karl-Schwarzschild-Strasse 2, W-8046 Garching bei München, Federal Republic of Germany
[5] Institut d'Astrophysique, Université de Liège, Avenue de Cointe, 5, B-4200 Cointe-Ougree, Belgium

Received June 13, accepted July 23, 1991

Abstract Deep optical imaging and spectroscopy have been obtained for the well known radio Einstein ring MG1131+0456 with the ESO/NTT. The direct CCD frames show a red emission excess at the exact location of the radio ring. Subsequent subtraction of the lensing galaxy, assumed to be an elliptical galaxy, results in the detection of an optical ring which is strikingly similar to the radio ring. Gravitational lensing models, including source reconstruction, predicts that the source is likely a radio-galaxy for which both the optical and extended radio emissions are sufficiently distorted by the foreground lensing galaxy as to produce a nearly complete ring. Our spectroscopy and broad band photometry suggest that the lensing galaxy has a spectral energy distribution typical of a non evolved elliptical, tentatively at z=0.85. The radio-galaxy associated with the radio-ring is likely to be an elliptical at larger redshift, tentatively z=1.13.

Keywords: cosmology — gravitational lenses — galaxies: general — MG1131+0456

1. Introduction

Since the discovery of the first gravitational mirage for the QSO 0957+561 by Walsh et al (1979), observers have identified a large variety of lensing phenomena. The most striking examples are the splitting of QSOs into four images (e.g. Huchra et al, 1985; Magain et al, 1988), the gravitational distortion of faint distant galaxies into giant arcs by foreground rich clusters (Lynds and Petrosian, 1986; Soucail et al, 1987) and the nearly perfect Einstein rings detected at radio wavelengths (Hewitt et al, 1988; Langston et al, 1989). Obviously the unusual morphologies observed for the above images were at the basis of their identifications as gravitational lensing events. They probably correspond to the top and visible tail of the lensing phenomena —strong lensing events — and it is very likely that a larger number of (still) unknown lensing events remain to be discovered.

Radio ring observations fit well with this idea. They are likely caused by the close alignment between a distant extended radio source and a foreground and massive lensing galaxy. They illustrate well the early prediction by Zwicky (1937) that massive galaxies constitute efficient lenses. However, such phenomenon would be nearly impossible to detect at optical wavelengths because the Einstein ring (radius smaller than 1" if the lensing galaxy mass is about $10^{12} M_{\odot}$ and lies at z= 0.5) should be blended with the lensing galaxy image (Hammer, 1987). At radio wavelengths, beautiful rings are produced by radio quiet lensing galaxies. Two such rings were discovered by means of a systematic survey of more than 6000 sources carried out with the VLA (Bennett et al., 1986). As stated by Kochanek (1991), the low rate of success is probably due to observational limits. Indeed, radio sources are expected to be affected by lensing because of the steep slope of the radio luminosity function, especially at its brightest end. The reality of such effects was demonstrated statistically from observations of a sample of high redshift galaxies from the 3CR catalog for which an excess of foreground massive galaxies and clusters has been found (Hammer and Le Fèvre, 1990).

We present in this letter new optical observations of the field around the radio ring MG 1131+0456, obtained with the ESO/NTT in the course of the "gravitational lensing" ESO key program.

2. Observations

2.1 Detection of the optical counterpart of MG1131+0456

The deflecting galaxy was readily identified by Hewitt et al. (1990) and by Gladisher et al. (1990, preprint), and we set to obtain better S/N in order to detect the optical counterpart of the source. Images of the field around MG1131+0456, in B, V, R, and Gunn *i*, were taken in February and May 1990 with the ESO/NTT and the imaging spectrograph EFOSC2 with a 1024^2 pixels Thomson CCD providing a plate scale of 0.164 arcsec/pixel. Exposures of 20 min in B, 20 min in V, 75 min in R and 55 min in Gunn *i* were taken under photometric conditions and with an image quality between 0.7 and 1.0 arcsec FWHM, as measured on the individual frames. Only an upper limit to the B magnitude of the optical counterpart of MG11331+0456 could be derived, due to the faintness of the source and because of the poor CCD sensitivity in the blue spectral range. However, the source was clearly detected in V, R and Gunn *i*: Figures 1 a to c show the final processed (and co-added when applicable) CCD frames as well as the sum of the R and *i* images. We measured the following magnitudes, as derived from observations of standard stars in the E3 and E5 fields (Graham, 1982), B>25, V=22.66±0.25, R=22.14±0.07, *i*=20.67±0.08.

It is clearly obvious, particularly from the R and *i* images, that the optical image of MG1131+0456 is quite extended and different from what is expected for the surface brightness of normal galaxies. Of special interest is the surface brightness excess observed at a distance 1.0<r<2.1 arcsec from the central peak, corresponding to the expected location of the radio ring. Figure 2 shows a radial plot of the pixel intensities observed in the sum of the R and Gunn *i* images; the emission excess is apparent at a distance between 1.0 and 2.1 arcsec from the peak emission at flux levels of μ_{R+i}=24.1 mag/arcsec^2 (S/N>5). One can also note that this flux excess increases from V to *i*.

* Based on observations obtained at the European Southern Observatory, La Silla, Chile in the framework of the "gravitational lensing" key program.
** Also, Chercheur Qualifié au Fond National de la Recherche Scientifique (Belgium)

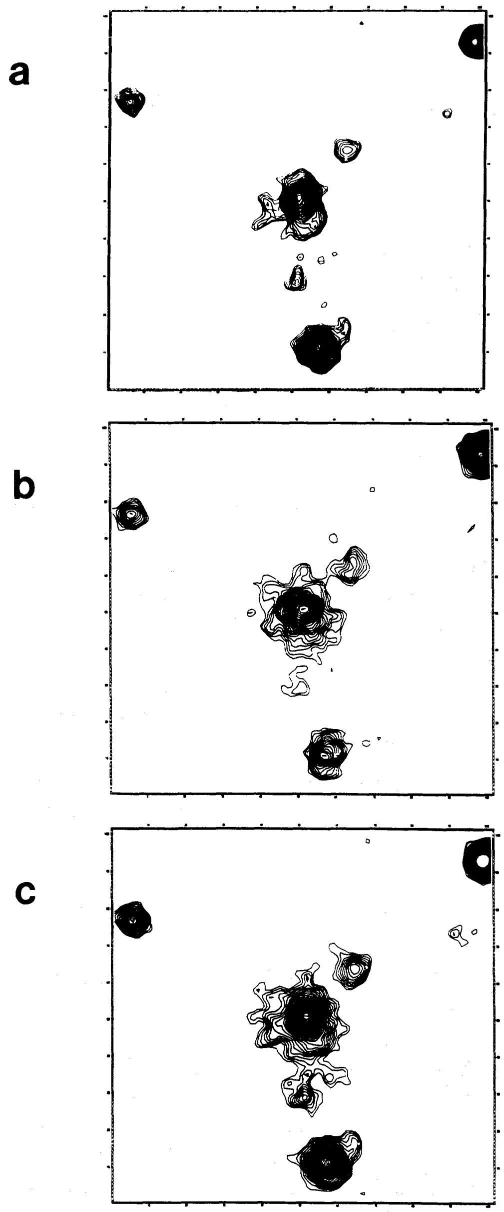

Figure 1 MG1131+0456 ESO/NTT direct imagery: *(a)* Sum of the R images, 75 min total integration, FWHM=0.80"; *(b)* Sum of the *i* images, 55 min. total integration, FWHM=0.95"; *(c)* Sum of the R and *i* images

To better show the spatial location of this luminosity excess, we built a galaxy model image with a $r^{1/4}$ luminosity profile that we later subtracted from the data. We set the peak intensity the same as the central peak intensity of the MG1131+0456 optical counterpart, and we built a set of galaxy models with axis ratios between 0.5 and 1.0 and position angles between 0 and 90° (every 15°), each with effective radii between 0.25 and 1 arcsec (2.5 to 10 kpc if the deflector is at z˜0.85, see below). We then subtracted it from our R+*i* image. The best fit to the data was produced for $0.4<r_{eff}<0.6$ arcsec with an axis ratio of 0.8 and a position angle of 36° NW. One must note that by increasing r_{eff}, it was not possible to subtract satisfactorily both the central emission and the emission excess between 1 and 2.1 arcseconds from the peak, and that the model fit to the data was degraded both for the inner 1 arcsec radius and for radii larger than 2.1 arcsec. The result of subtracting a galaxy model with r_{eff}=0.5 arcsec, with a magnitude *i*=21.4, which provides the best fit to the data, is shown in Figure 3, and the corresponding luminosity profile is plotted in Figure 2. Hubble profiles were also used to built model galaxies: they provided slightly worse fit to the data (Figure 2). The residual emission has the shape of a ring, with a S/N of 3 to 10, and an integrated magnitude *i*=21.5. It shows a morphology and location very similar to the radio ring: in particular the North-West gap in the optical emission matches very closely the gap observed in the radio emission (see Figures 1 and 2 in Hewitt et al., 1988). This indicates that the source is an extended object, probably a radio-galaxy. Note that the model parameters for the deflecting galaxy have been checked for consistency against the parameters derived from the gravitational lensing modelling: they are very close to what was used in the model of Kochanek et al. (1989) as well as to our model parameters (see section 3).

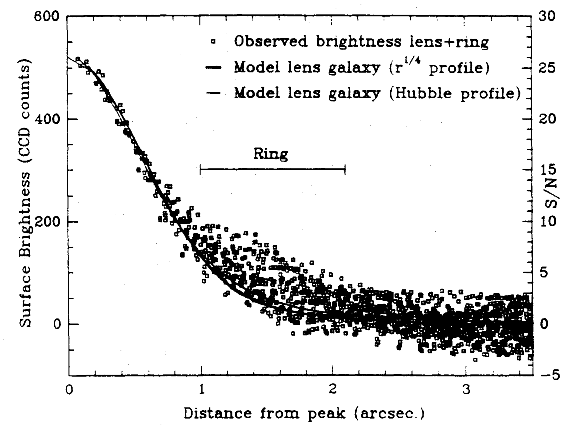

Figure 2 Radial plot of the pixel's intensities in the R+*i* image, centered on the peak intensity. Note the presence of a light excess for radii between 1 and 2.1 arcsec. The best elliptical galaxy model shown as the heavy solid line was built with a $r^{1/4}$ luminosity profile with r_{eff}=0.5", the light line is the best galaxy model built with a Hubble profile; both of them convolved with the PSF

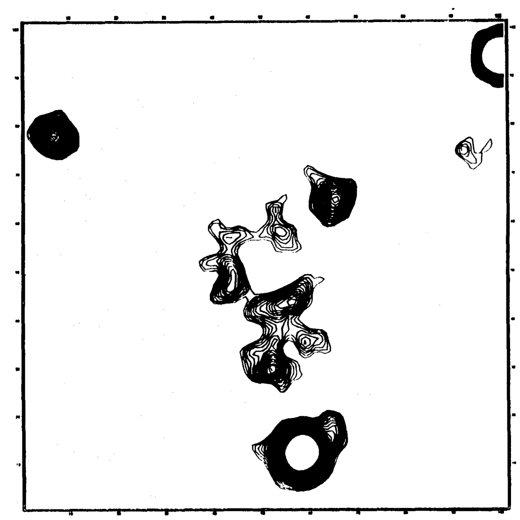

Figure 3 Result of the subtraction of an elliptical galaxy model with a $r^{1/4}$ luminosity profile with r_{eff}=0.5", an axis ratio of 0.8 at a P.A. of 36° NW. The residual image has the shape of a ring; note the gap to the NW, corresponding to the gap observed in the radio ring. The lowest isophote has a S/N=3, and the S/N is increasing by 0.3 between successive isophotes

2.2 Spectroscopy

Low resolution spectroscopy was obtained in February 1990. A red grism provided a spectral coverage between 5000Å and 9300 Å, and a slit of 1.1 arcsec (indicated on figure 1.b) produced an instrumental resolution of ˜50 Å. Integrations of twice 40 min and 30 min were obtained under photometric conditions with an image quality of 0.9" FWHM, the location of the object on the CCD being shifted by ˜10 arcsec between successive exposure. Spectra were processed in a standard way using the NOAO/longslit package within the NOAO/IRAF data reduction facilities, and were registered and then co-added to produce the final spectrum displayed in figure 4.

The spectrum of the optical emission associated with MG 1131+0456 is probably due to the blend of both the lens and source spectra: it is featureless, no emission lines are present between 5000 Å and 9300 Å, but it shows a very red continuum consistent with our photometric results. We tentatively note the presence of two breaks in the red part of the continuum at 7400 Å and at 8550 Å. Although their significance are low (S/N ˜ 2–2.5), they are not simple artifacts due to the sky-substraction. The recorded spectrum is similar to the spectra of bright ellipticals in distant clusters (z= 0.70– 0.92, Oke, 1984) as well as to the spectrum of the lensing galaxy (z = 1.01) responsible for the multiple images of the QSO 2016+112 (Schneider et al, 1986). The photometric data from B to I suggest changes of the continuum slope between the V and R filters, and even more between the R and I filters and therefore supports the spectroscopic data. The V image is compact, and shows no or little extra emission at the location of the radio ring. It also shares the same peak location as in the other colors. Taken altogether, these properties suggest that the lens spectrum may be responsible for the break at 7400 Å and could be an elliptical galaxy at z= 0.85. This hypothesis is highly consistent with the lensing scenario since: (i) the lens should be a massive galaxy in order to distort gravitationally the background radio source (see next section); (ii) our best substraction is provided for a r_{eff}=5kpc elliptical lens with R= 22.6, which would correspond at z=0.85 to M_B= —21.7 (k-corrected, H_0= 50 km/s/Mpc); (iii) ellipticity and P.A. of the V image are consistent with what Kochanek et al (1989) needed in order to reproduce the north-west gap in the radio ring at 15 GHz.

The absence of emission lines excludes that the MG 1131+0456 source is a radio-galaxy similar to the distant and powerful radio-galaxies as found in the 3CR catalogue. Moreover, the excess of emission associated with the optical ring is much more significant in the I filter than in the R filter. Therefore the background radio-galaxy is likely a radio loud elliptical which might be at z=1.13 if one associates the 8550 Å break with the 4000 Å break at rest. Such a redshift for the source is very speculative and need confirmation from further observations.

3. Reconstruction of the optical and radio sources: lensing model

The gravitational lensing model used here is described by Hammer and Rigaut (1989). The lensing galaxy is assumed to follow a $r^{1/4}$ surface density profile and to be located at z=0.85. Homoeidal symmetry (Schramm, 1989) allows our model to account for the ellipticity of the lensing mass distribution without any a priori assumptions on the associated potential (Angonin et al, in preparation). The first step is to estimate the lensing parameters from the modelling of the radio ring: for simplicity we have assumed a core plus jet morphology for the source (assumed to be at z=1.13). Other combinations of lens and source redshifts would simply change the characteristic lensing mass by a scaling factor. Figure 5 shows the result of the model which best fits the radio ring at 5 GHz (Hewitt et al, 1988). However, similarly to the Kochanek et al. (1989) results, either the modeled ring is too round or the splitting of the radio core is not well reproduced. This

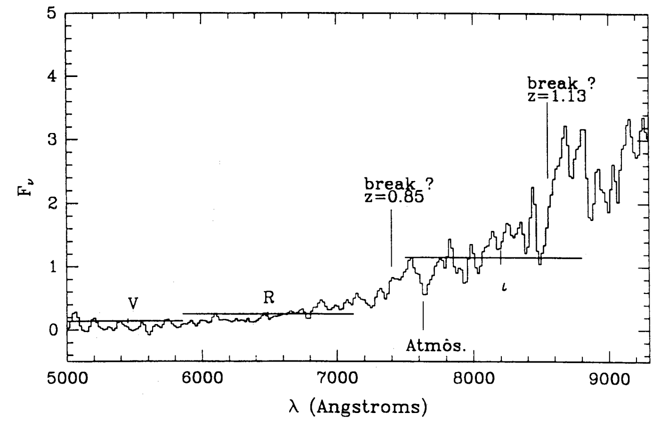

Figure 4 ESO/NTT spectrum recorded for the optical counterpart of MG1131+0456. The total integration time was 110 min. The horizontal bars represent the relative flux levels as derived from our photometric data

may arise because of the presence of another lens such as a cluster around the lensing galaxy, but not centered on it. No evidence for such a cluster had been found from our deep R and *i* exposures, although these bandpasses are not well suited to identify a z∼0.8 cluster. The following step was to use this model to fit the optical ring and then reconstruct the optical source. We have improved our numerical model by adding a procedure of source image reconstruction similar to the one described by Kochanek et al. (1989). Image pixels and their intensity have been picked up from the sum of our R and *i* CCD images; only pixels with a S/N>3 have been used. Figure 6 shows the reconstructed image of the optical source, using the same set of parameters as in Figure 5. The optical source morphology appears to be consistent with that of an elliptical galaxy (r_{eff}= 0.5") at large z. Our image analysis lead to a reliable estimation for the optical ring magnitude, *i*= 21.5±0.3, and, although more difficult to estimate R=23.3±0.7. Our modelling provides a magnification factor of about 5–8 and the unlensed radio galaxy would be seen as a *i*= 23.5– 24 galaxy, at least 3 magnitudes fainter than the powerful 3CR radio-galaxies at z > 1. Indeed, the residual radio source is at least ten times less powerful than high-redshift 3CR radio sources: its radio-flux is lower than 40 mJy at 5 Ghz and lower than 8 mJy at 15Ghz after correction for the magnification factor. Another interesting consequence of our modelling is the possibility of deriving the accurate location of the reconstructed optical source relative to the radio source. Indeed, as was pointed out by Kochanek et al. (1989), the location of the lens center is well constrained by the model of the radio ring within an accuracy of about ±0".2. On the other hand, we find that the optical ring is well reproduced by setting the lens center at the peak of the optical emission, which is known down to an accuracy of ±0".1. Gravitational lensing of both the radio and optical galaxy leads to an astrometry for the reconstructed source down to an accuracy of less than ±0".3 with respect to the radio coordinate frame (see Figure 6).

4. Conclusions

New optical observations of the radio ring MG 1131+0456 have been presented. Both observing and modelling could have helped us to disentangle the source properties (the radio galaxy) from the lensing mass properties (the foreground elliptical and maybe a cluster). However, we have found that radio rings are not a very powerful mean to investigate the lensing mass distribution. Numerical simulations based on varying the lensing parameters in a four dimensional space (mass, effective radius, ellipticity and a single parameter for the virtual source location) left open

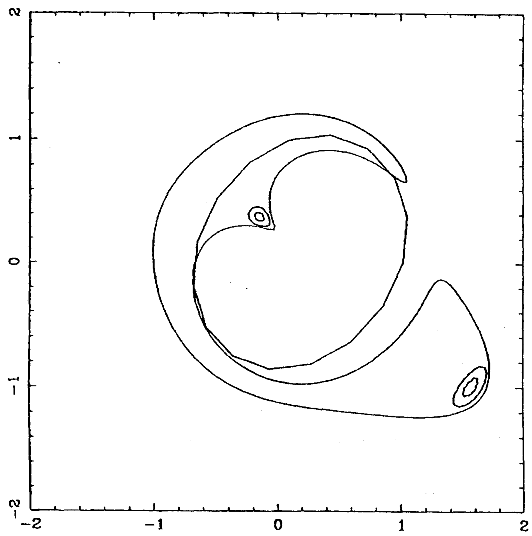

Figure 5 Lensing model reconstruction of the radio ring at 5 GHz. The source was assumed to have a core + jet morphology. Parameters used here are: M=2.5x10$^{12}M_\odot$ for r_{eff}=0"5 and an axis ratio of 0.8 for P.A.=30°NW. Our simulations show that the P.A. is well constrained within 20° in order to reproduce the NW gap of emission, while the axis ratio should be between 0.4 to 0.8. However, by using several combinations of (M, r_{eff}), we did not find any strong constraint on the mass distribution as the mass inside the ring is 1.3x10$^{12}M_\odot$

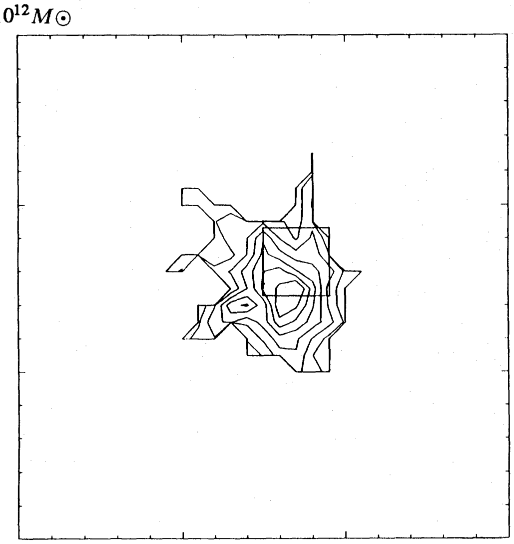

Figure 6 Lensing model reconstruction of the optical ring from the R+i images. Same set of parameters as in Figure 5. The square box indicates the location of the radio core as inferred from the accurate astrometry provided by the lensing configuration (see text)

a very large set of possibilities, especially for the lensing mass distribution. Indeed the ring thickness is too large and prevents one against the possibility to set the location of critical lines, contrary to the case of the giant thin and luminous arcs in rich clusters (Hammer and Rigaut, 1989).

However, observations of radio rings might help us to catch a population of radio-galaxies which would be far beyond the scope of the largest telescopes without the help of the gravitational lensing magnification factor. Our excellent seeing images have led to the detection of the optical source associated with the radio ring MG 1131+0456 with a ring-like morphology. Properties of the radio and optical source can be investigated after correcting for the magnification factor, for which there is an uncertainty by a factor 2 in our modelling. The radio source is found to be at least 15 times less powerful than the high-redshift 3CR radio-sources and the optical counterpart appears to be at least 3 magnitudes fainter than 3CR galaxies of comparable redshift. Indeed the MG 1131+0456 optical counterpart does not show any sign of strong emission line activity which would be expected if the rough correlation between emission line activity and radio power (Spinrad, 1986) was extended down to mJy levels. The source of M1131+0456 could be a moderately luminous elliptical (L∼L*), without any sign of strong star formation, while the radio emission dominates the whole energy spectrum. The way this object has been discovered indicates that it belongs to a relatively abundant population of sources with properties very different from the uncommon and very powerful radio-galaxies at high redshifts selected in the 3CR (9Jy at 178 MHz) or 1Jy samples (at 408 MHz, Allington-Smith, 1982). It would be interesting by several aspects to carry on K band observations of this system at high spatial resolution.

Analysis of our data combined with the lensing model show that the lensing galaxy of the MG 1131+0456 system is very likely a massive elliptical, tentatively at z=0.85. This might be another example of a massive galaxy at relatively high redshift which does not show any evidence for strong evolution (or star formation activity) and which can be compared with the lensing galaxy of the gravitational mirage QSO 2016+112 (Schneider et al, 1986). Deeper spectroscopic measurements are needed to confirm the redshifts of the source and lens.

Acknowledgments

The research of Jean Surdej in Liège is partially supported by contract ARC90/94–140 "Action de recherche concertée de la communauté Francaise" (Belgium).

References

Allington-Smith, J.R., 1982, MNRAS, 199, 611
Bennett, C. L., Lawrence, C. R., Burke, B. F., Hewitt, J. N., Mahoney, J., 1986, Astrophys. J. Suppl. Ser., 61, 1
Graham, J.A., 1982, P.A.S.P., 94, 244
Hammer, F., 1987, in 3rd IAP Astrophys. Meeting on High Redshift Objects, Ed. Bergeron et al, Frontieres, P. 467
Hammer, F., Le Fèvre, O., 1990, Astrophys. J. 357, 38
Hammer, F., Rigaut, F., 1989, Astron. Astrophys., 226, 45
Hewitt, J. N., Turner, E. L., Schneider, D. P., Burke, B. F., Langston, G. I., Lawrence, C. R., 1988, Nature, 333, 537
Huchra, J. P., Goreinstein, M., Kent, S., 1985, Astron. J., 90, 691
Kochanek, C. S., Blandford, R. S., Lawrence, C. R., Narayan, R., 1989, M. N. R. A.S., 238, 43
Kochanek, 1991, preprint
Langston, G. I., Schneider, D. P., Conner, S., Carilli, C. L., Lehar, L., Burke, B. F., Turner, E. L., Gunn, J. E., Hewitt, J. N., 1989, Astron. J., 97, 1283
Lynds, R., Petrosian, V., 1986, Bull. Am. Astron. Soc. 18, 1014
Magain, P., Surdej, J., Swings, J. P., Borgeest, U., Kayser, R., Kuhr, H., Refsdal, S., McCarthy, P.J., Kapahi, V.K., van Breugel, W., Subrahmanya, C.R., Astron. J., 100, 1014
Remy, M., 1988, Nature, 334, 325
Oke, J. B., 1984, in "Clusters and Groups of Galaxies", Eds Mardirossian et al, Reidel Publishing Company, P. 99
Schneider, D. P., Gunn, J. E., Turner, E. L., Lawrence, C., Hewitt, J. N., Schmidt, M., Burke, B. F., 1986, Astron. J., 91, 991
Soucail, G., Mellier, Y., Fort, B., Picat, J. P., 1987, Astron. Astrophys., 172, L14
Spinrad, H., 1986, P. A. S. P., 98, 269
Walsh, D., Carswell, R., Weymann, R., 1979, Nature, 279, 381
Zwicky, F., 1937, Phys. Rev., 51, 290